Perspectives in using Raman spectroscopy for characterizing the microstructure of plutonium-bearing materials

Laeticia Medyk, Patrick Simon, Aurélien Canizarès, Dario Manara, Rudy J.M. Konings, Jean-Yves Colle, Romain Vauchy, Christophe Valot, Gilles Montagnac, Philippe M. Martin

Perspectives in using Raman spectroscopy for characterizing the microstructure of plutonium-bearing materials

Laetitia Medyk[1], Patrick Simon[2], Aurélien Canizares[2], Dario Manara[3], Rudy J. M. Konings[3], Jean-Yves Colle[3], Romain Vauchy[1], Christophe Valot[1], Gilles Montagnac[4], Philippe M. Martin[1]

[1]*CEA, Nuclear Energy Division, Research Department on Mining and Fuel Recycling Processes, SFMA/LCC, 30207 Bagnols-sur-Ceze, France*
[2]*Conditions Extremes et Materiaux : Haute Temperature et Irradiation (CEMHTI) - CNRS :UPR3079 - CS 90055 45071, 45071 Orleans, France*
[3]*European Commission, Joint Research Centre (JRC), Postfach 2340, 76125 Karlsruhe, Germany*
[4]*Laboratoire de Géologie de Lyon, CNRS, ENS de Lyon, 69364 Lyon, France*

INTRODUCTION

In the frame of the development of uranium-plutonium mixed oxide fuels for Sodium-cooled Fast Reactors (SFRs), characterizing nuclear materials by various techniques is paramount.
These fast neutron reactors imply the use of a $(U,Pu)O_{2-x}$ ceramic fuel with a Pu/(U+Pu) content between 19 and 30 mol.%. Furthermore, the physico-chemical and microstructural properties of such fuels, such as chemical homogeneity, oxygen stoichiometry (O/(U+Pu) ratio) and crystallographic structure, have to meet precise criteria for being introduced in the reactor core.
As evidenced in numerous studies by various experimental techniques, a supplementary difficulty with such high plutonium content is the existence of a miscibility gap comprised within the UO_2-PuO_2-Pu_2O_3 region[1,2]. Its presence is conditioned by the difference in the possible oxidation states adoptable by the two constituting cations. The miscibility gap itself is composed of three sub-domains, consisting in closely related cubic-type phases and its extent is a function of Pu content and temperature. The temperature of phase separation, *i.e.* the temperature at which this bi- (or tri-) phasic domain appears, depends on the oxygen to metal ratio (hereinafter O/M ratio) of the material. Recent high temperature X-ray diffraction (HT-XRD) studies allowed observing *in situ* the phase separation occurring in oxygen-hypostoichiometric uranium-plutonium mixed oxides with high plutonium contents[3–5].
Nevertheless, HT-XRD characterizations on $(U,Pu)O_{2-x}$ were performed on powder and thus did not allow observing *in situ* the microstructure changes induced by the phase separation phenomenon[3,4].
As highlighted by recent studies by Talip *et al*[6] and Elorrietta *et al*[7], Raman microscopy is a promising tool for characterizing the physico-chemical properties such as, among many others, the cation distribution homogeneity, the grain size, the crystal defects that are of main interest for the production of nuclear fuels.
The development of a new *in situ* Raman device dedicated to handling transplutonium-bearing materials is currently in progress in our laboratory (ATALANTE facility, CEA Marcoule, France).
We propose to present at the Plutonium Futures 2018 conference our first results obtained on $U_{0.75}La_{0.25}O_{2-x}$ and *in situ* high temperature measurements on CeO_{2-x} as the authorization of handling plutonium-bearing materials is not obtained yet. By the time of the conference and thanks to the fruitful collaboration existing between JRC Karlsruhe and our laboratory, we will be able to present our first results on $(U,Pu)O_{2-x}$ samples as well.

RESULTS

The results bellow were obtained on a $U_{0.75}La_{0.25}O_{2-x}$ sintered pellet. The sample was prepared by gel-supported precipitation, also referred as sol−gel external gelation[8]. The whole preparation route is presented elsewhere[9].
The following SEM picture (Fig. 1.) shows the microstructure of the polished $U_{0.75}La_{0.25}O_{2-x}$ sintered pellet. The estimated mean grain size is <5 µm.

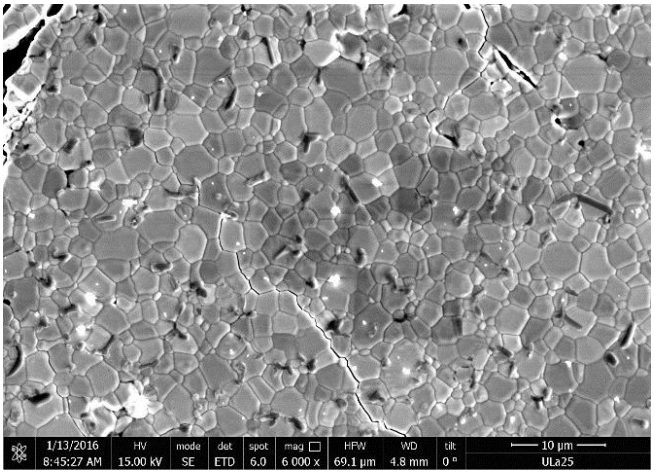

Fig. 1. SEM picture of the $U_{0.75}La_{0.25}O_{2-x}$ sintered pellet

The following Raman imaging measurements were performed at CEMHTI, Orléans, France using an InVia Reflex Renishaw system with a 514 nm LASER source (5mW and x50 objective). A 1 µm step size was used to

obtain 100x100 µm Raman maps. The Figure 2. represents a fake colored intensity map of the T_{2g} line superimposed with the optical image.

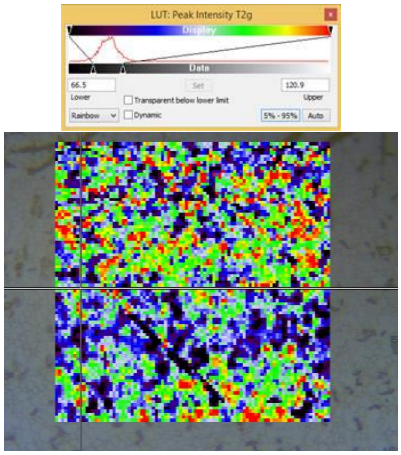

Fig. 2. Map of the Raman T_{2g} intensity line (fake colors) obtained on $U_{0.75}La_{0.25}O_{2-x}$ (100x100 µm)

As shown by Maslova *et al.*[10] on UO_2 sample, a part of the T_{2g} intensity inhomogeneities is due to different orientations of the ceramic grains that allows observing the microstructure itself (grain boundaries, microstructural defects, *etc*). Thus, as revealed here, the methodology established on UO_2 can applied to mixed oxides.

In a second part, we will present our results obtained by *in situ* Raman (532 nm laser source at LGL of ENS Lyon, France) on CeO_{2-x} samples using a nuclearized version of Raman micro furnace developed by Montagnac *et al.*[11]. Furthermore, this unique device is associated with a setup allowing measuring, imposing and monitoring the variations in the oxygen partial pressure during a given heat treatment. As shown in Figure 3, a significant shift in the T_{2g} line is observed as a function of temperature related to the lattice thermal expansion. Moreover, both the intensity loss and the line broadening are induced by thermal agitation of anionic sublattice.

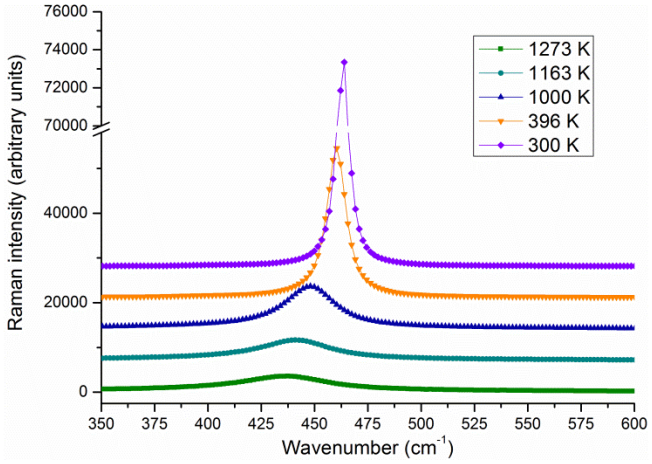

Fig. 2. Variation in the Raman spectra (T_{2g} line) of CeO_2 with temperature in air

The same experiments were performed on a similar sample in reducing conditions ($pO_2 = 1.10^{-15}$ bar) up to 1420 K. the magnitude of the shift previously observed on the T_{2g} line position was larger under these conditions. This phenomenon is explained by the *in situ* reduction of stoichiometric CeO_2 to oxygen-hypostoichiometric CeO_{2-x}. We hope this promising result could be useful for determining the O/M ratio of the materials studied as a function of the thermodynamic conditions (T and pO_2).

Finally, uranium-plutonium mixed oxide samples with 19 mol.% Pu are being characterized at JRC Karsruhe with the experimental setup described in ref[12]. Experiments are performed on sintered pellets, manufactured by powder metallurgy, and show variations in the T_{2g} line position as a function of the local plutonium concentration. Raman mapping of such samples are planned in the near future.

REFERENCES

1. T. L. MARKIN and R. S. STREET, "The uranium-plutonium-oxygen ternary phase diagram," J. Inorg. Nucl. Chem. **29** 9, 2265 (1967); https://doi.org/10.1016/0022-1902(67)80281-1.
2. C. SARI, U. BENEDICT, and H. BLANK, "A study of the ternary system UO2-PuO2-Pu2O3," J. Nucl. Mater. **35** 3, 267 (1970); https://doi.org/10.1016/0022-3115(70)90211-4.
3. T. TRUPHÉMUS et al., "Structural studies of the phase separation in the UO2–PuO2–Pu2O3 ternary system," J. Nucl. Mater. \b432 1, 378 (2013)
4. R. VAUCHY et al., "High temperature X-ray diffraction study of the kinetics of phase separation in hypostoichiometric uranium–plutonium mixed oxides," J. Eur. Ceram. Soc. **34** 10, 2543 (2014); https://doi.org/10.1016/j.jeurceramsoc.2014.02.028.
5. R. C. BELIN et al., "In situ high temperature X-Ray diffraction study of the phase equilibria in the UO2–

PuO2–Pu2O3 system," J. Nucl. Mater. **465**, 407 (2015); https://doi.org/10.1016/j.jnucmat.2015.06.034.
6. Z. TALIP et al., "Characterization of un-irradiated MIMAS MOX fuel by Raman spectroscopy and EPMA," J. Nucl. Mater. \b499, 88 (2018)
7. J. M. ELORRIETA et al., "Raman study of the oxidation in (U, Pu)O2 as a function of Pu content," J. Nucl. Mater. \b495 Supplement C, 484 (2017)
8. U. CARVAJAL-NUNEZ et al., "Charge Distribution and Local Structure of Americium-Bearing Thorium Oxide Solid Solutions," Inorg. Chem. **51** 21, 11762 (2012); https://doi.org/10.1021/ic301709d.
9. D. PRIEUR et al., "Aliovalent cation Substitution in UO2: Electronic and Local Structures of U1–yLayO2±x Solid Solutions," Inorg. Chem. (2018); https://doi.org/10.1021/acs.inorgchem.7b02839.
10. O. A. MASLOVA et al., "Raman imaging and principal component analysis-based data processing on uranium oxide ceramics," Mater. Charact. **129**, 260 (2017); https://doi.org/10.1016/j.matchar.2017.05.015.
11. G. MONTAGNAC et al., "Anharmonicity of graphite from UV Raman spectroscopy to 2700K," Carbon **54**, 68 (2013); https://doi.org/10.1016/j.carbon.2012.11.004.
12. M. NAJI et al., "An original approach for Raman spectroscopy analysis of radioactive materials and its application to americium-containing samples," J. Raman Spectrosc., n/a (2015); https://doi.org/10.1002/jrs.4716.